
Efficient Preference-Based Reinforcement Learning Using Learned Dynamics Models

Yi Liu
UC Berkeley

Gaurav Datta
UC Berkeley

Ellen Novoseller
Army Research Lab

Daniel S. Brown
University of Utah

Abstract

Preference-based reinforcement learning (PbRL) can enable robots to learn to perform tasks based on an individual’s preferences without requiring a hand-crafted reward function. However, existing approaches either assume access to a high-fidelity simulator or analytic model or take a model-free approach that requires extensive, possibly unsafe online environment interactions. In this paper, we study the benefits and challenges of using a *learned dynamics model* when performing PbRL. In particular, we provide evidence that a learned dynamics model offers the following benefits when performing PbRL: (1) preference elicitation and policy optimization require significantly fewer environment interactions than model-free PbRL, (2) diverse preference queries can be synthesized safely and efficiently as a byproduct of standard model-based RL, and (3) reward pre-training based on suboptimal demonstrations can be performed without any environmental interaction. Our paper provides empirical evidence that learned dynamics models enable robots to learn customized policies based on user preferences in ways that are safer and more sample efficient than prior preference learning approaches.

1 Introduction

Developing assistive and collaborative robots that adapt to a variety of end-users requires customizing robot behaviors without manually tuning cost functions. One approach is for robots to learn from human demonstrations [1]. However, providing demonstrations is not always possible and when demonstrations are suboptimal, existing methods often overfit to the suboptimalities [16, 10, 34].

Rather than rely on demonstrations, preference-based reinforcement learning (PbRL) approaches query the user for pairwise preferences over trajectories [48]. However, existing approaches either use model-free PbRL and assume access to a perfect simulator [14] or take a model-based approach, but assume access to an analytic model [41] of the dynamics. In many problems, however, a good dynamics model is not available and must be inferred from data, as done in model-based reinforcement learning (RL). However, prior work on PbRL has not addressed the challenges and potential benefits of using a learned dynamics model to perform PbRL. Due to the importance of model-based RL in robotics domains, we propose to study Model-based Preference-based RL (MoP-RL). To our knowledge, this work performs the first study of the benefits of learning a dynamics model for learning from preferences. *Central to our paper is the idea that combining model-based RL techniques with human preference learning offers the following advantages: 1. Safer and more sample efficient reward learning and policy optimization. 2. Diverse trajectories useful for preference learning, which arise as a free byproduct of model-based RL. 3. Reward pre-training with automatically generated preferences over demonstrations without any environmental interactions.*

Safe and sample efficient learning. Combining model-based RL with PbRL allows robots to use a learned dynamics model to learn customizable behaviors; in particular, the algorithm can hypothesize different behaviors and even show these planned behaviors to a human without executing them in

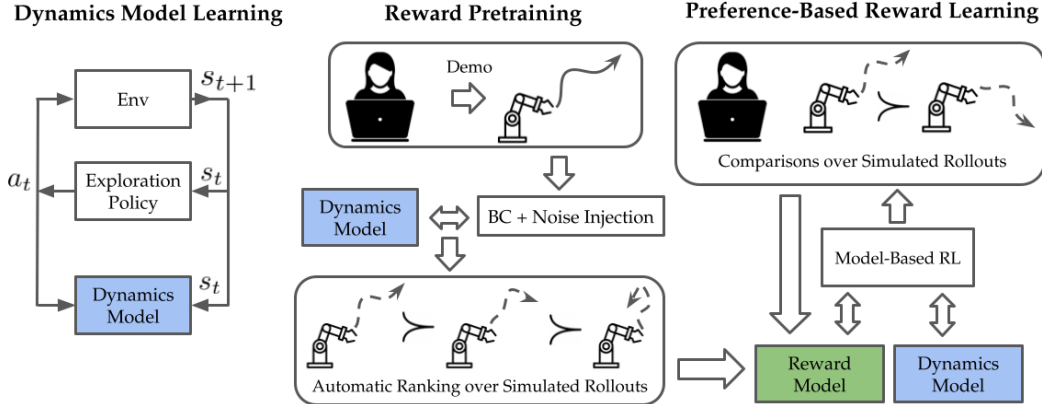


Figure 1: **Model-based Preference-based RL (MoP-RL)**: Our pipeline enables sample efficient human preference learning using a learned dynamics model. First, we leverage intrinsic exploration to learn a dynamics model. This enables efficient reward pre-training by running behavioral cloning (BC) on a small number of demonstrations and injecting varying degrees of noise into the BC policy to simulate trajectories with the learned dynamics. We then fine-tune the learned rewards via active preference queries to a human, where the queried trajectories are simulated using the learned dynamics model and produced as a byproduct of model-based RL with the learned reward function.

the environment. This enables safe and efficient reward function learning and policy optimization by limiting the requisite number of environmental interactions. Though learning a dynamics model may require a large amount of data, this does not require human time, and furthermore, we may amortize the cost by learning multiple reward functions for different users, leveraging the same learned dynamics model. This is critical for application of PbRL methods: because model-free methods are comparatively data hungry in terms of agent-environment interaction steps, they can be difficult to deploy in real-world domains such as robotics.

Diverse trajectories for preferences learning. A learned dynamics model can also be used to generate informative preference queries with diverse trajectories, without any environment interaction. To decide which trajectories to show to the human, we note that model-based RL provides a diverse set of trajectories, useful for preference queries, without any extra computation. Given the learned dynamics model, we use model predictive control (MPC) to optimize trajectories. One common MPC approach is to use a cost function (learned from preferences in our case) to iteratively refine an action sequence [46, 21, 15, 18, 26, 35]. We use the cross entropy method (CEM) [7] and show that the trajectories generated by successive CEM iterations provide a diverse set of trajectories that can be reused for preference learning. In addition, successive iterations of CEM with a learned reward function will converge to the model’s best guess of the human’s preference. Obtaining preference queries over successive CEM iterations allows the supervisor to quickly correct the learned reward function if it leads to undesired behavior.

Reward pre-training from suboptimal demonstrations. Learned dynamics models additionally enable reward pre-training without any need to collect samples from the environment. Prior work has proposed methods for learning rewards from suboptimal demonstrations by injecting noise into a learned policy [11, 13]. We extend Disturbance-based Reward Extrapolation (D-REX) [11], which injects noise into a policy learned via behavioral cloning. While this approach has been shown to learn reward functions that enable better-than-demonstrator performance, D-REX requires rolling out noisy trajectories, which can be unsafe. However, with a learned dynamics model, we can perform such noisy rollouts within the model. We study this approach and show that even with suboptimal demonstrations, we can achieve a significant speed-up in preference learning using model-based reward pre-training.

This work contributes: 1. The first analysis of preference-based RL with a learned dynamics model, via the proposed MoP-RL framework (see Figure 1). 2. A novel preference generation approach that uses the trajectories produced as a byproduct of model-based RL to generate diverse and informative preference queries without requiring physical rollouts in the environment. 3. An approach for

reward pre-training together with MoP-RL, which enables combining suboptimal demonstrations and pairwise preferences in a model-based setting. 4. Experiments suggesting that our approach can learn to perform complex tasks from preferences with fewer environment interactions than prior approaches and can scale to high-dimensional visual control tasks.

Code and supplemental material are available at <https://sites.google.com/berkeley.edu/mop-rl>.

2 Related Work

Model-Based Learning. There has been much interest in learning dynamics models [36, 24, 42, 31] and applying these learned models to RL [15, 37, 56, 44, 54, 45, 4, 52, 53, 33]. Past work has indicated that model-based RL can achieve higher sample efficiency than model-free methods [29, 55]. Outside of RL, learned dynamics models have also been used successfully in imitation learning methods that learn from expert demonstrations. For instance, forward and inverse dynamics models have been shown to be useful when learning from demonstrations consisting of state-action pairs [22, 3, 2, 51], as well as when learning from observations without access to the demonstrator’s actions [43, 19, 30]. ReQueST [38] may be the most closely-related existing work to ours, as it actively collects human reward labels over model-based trajectory rollouts and performs model-based RL using a learned reward function. However, our work differs in the following important ways: (1) ReQueST only performs model-based RL on the learned rewards after completion of learning; in contrast, MoP-RL leverages the reward learned *so far* to synthesize human feedback queries using informed trajectories that improve throughout learning. (2) ReQueST requires a human to provide a reward label to every state in each queried trajectory, resulting in a significantly higher human burden than MoP-RL, which requires only pairwise preferences over entire trajectories.

Preference-Based RL. It is often easier for someone to qualitatively rank two or more behaviors than to demonstrate a good behavior. Learning from pairwise preferences over trajectories is a common approach to learning reward functions and corresponding RL policies. However, despite the widespread interest in preference-based RL, most prior work either takes a model-free approach [50, 14, 27, 9, 32] or assumes that the system dynamics are perfectly known [57, 47, 23, 49, 28, 41, 6]. In this paper, meanwhile, we seek to study preference-based RL when using a learned dynamics model. Prior works on model-free preference-based RL demonstrate the effectiveness of pairwise preference learning for a range of RL tasks [14, 10, 32]. In particular, PEBBLE [32] achieves state-of-the-art performance of PbRL in simulated robot locomotion and manipulation tasks. However, model-free RL tends to require more environment interaction than model-based RL methods [29, 55], and we are not aware of prior work that studies PbRL with dynamics model learning. Our experiments suggest that MoP-RL achieves better policy performance with significantly fewer environment interactions. Recent work by Chen et al. [13] provides evidence of inductive bias when pretraining using noise injection and a preference-learning objective, as done in our paper. However, Chen et al.’s approach requires solving a sequence of optimization problems and running online IRL, thus it requires a large amount of computation time and many on-policy rollouts [13]. We leave it for future work to investigate alternatives to D-REX [11] for reward pretraining without environmental interaction.

3 Problem Definition

Problem formulation and notation. We formulate the problem as a Markov Decision Process (MDP), $\mathcal{M} = (\mathcal{S}, \mathcal{A}, P, r)$, where \mathcal{S} is the state space, \mathcal{A} is the action space, $P : \mathcal{S} \times \mathcal{A} \times \mathcal{S} \rightarrow [0, 1]$ specifies the state transition probabilities, and r is the human’s reward function, which, importantly, we assume is unobserved by the learning agent. A *trajectory* of agent-environment interaction takes the form $\tau = (s_0, a_0, s_1, a_1, \dots, s_T)$ for some episode length T .

While the learning agent does not observe numerical rewards, we assume access to a human user who can answer pairwise preference queries of the form, “Do you prefer trajectory A or B?”, as well as possibly provide an initial set $\mathcal{D}_{\text{demo}}$ of suboptimal demonstrations, where $\mathcal{D}_{\text{demo}}$ consists of trajectories $\tau^E = (s_0^E, a_0^E, \dots, s_T^E) \in \mathcal{D}_{\text{demo}}$. The pairwise preference $\tau_A \succ \tau_B$ indicates that the user states a preference for trajectory τ_A over τ_B . We assume that the human’s preferences are based on a true but unobserved reward function, $r : \mathcal{S} \times \mathcal{A} \rightarrow \mathbb{R}$, which quantifies the utility of each

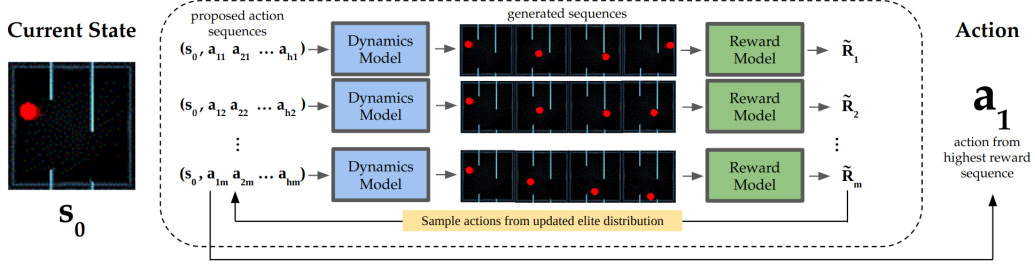


Figure 2: **Cross Entropy Method (CEM)**: For initial state s_0 , we sample a set of action sequences and for each, predict the corresponding state trajectory via the dynamics model \hat{f}_ϕ . We estimate these trajectories’ rewards as a linear combination of the reward model \hat{r}_θ ’s prediction and RND. The m_e action sequences with the highest predicted rewards form the elites; these are used to update the CEM distribution and sample the next action sequence set. After the final CEM iteration, the mean of the CEM distribution for the first action in the sequence is selected for execution in the environment.

state-action pair to the human. The total underlying reward of a trajectory $\tau = (s_0, a_0, s_1, a_1, \dots, s_T)$ is denoted via $J(\tau) := \sum_{t=0}^{T-1} r(s_t, a_t)$.

A *policy* $\pi : \mathcal{S} \times \mathcal{A} \rightarrow [0, 1]$ is a mapping from states to a distribution over actions. We aim to learn a policy π that matches user preferences by maximizing expected performance under the human’s true reward function r . Our only access to r is through the demonstrations and pairwise preferences.

Assumptions. We assume access to a human who can give preferences over trajectories based on their internal utility function as described above. As part of this assumption, we assume that we can visualize trajectories for the human to rank. Note that we only assume access to a method to show the human a sequence of states—we do not assume to know or have a model of the true system dynamics.

Performance metrics. We aim to identify the optimal policy π^* that maximizes the human’s total underlying reward in expectation: $\pi^* = \operatorname{argmax}_\pi \mathbb{E}_{\tau \sim \pi} [J(\tau)] = \operatorname{argmax}_\pi \mathbb{E}_{\tau \sim \pi} \left[\sum_{(s,a) \in \tau} r(s, a) \right]$. Furthermore, we aim to discover π^* while minimizing the total amount of environment interaction and the total number of human preference queries required.

4 Methods

Learning Rewards from Preferences. To obtain a well-performing policy π , we learn a predictor $\hat{r}_\theta : \mathcal{S} \times \mathcal{A} \rightarrow \mathbb{R}$ of the user’s reward r , parameterized by θ . We model the probability that the user prefers trajectory τ_1 to τ_2 via the Bradley-Terry model [10, 14]: $P(\tau_1 \succ \tau_2) \approx \frac{\exp(\hat{J}_\theta(\tau_1))}{\exp(\hat{J}_\theta(\tau_1)) + \exp(\hat{J}_\theta(\tau_2))}$, where $\hat{J}_\theta(\tau) := \sum_{s,a \in \tau} (\hat{r}_\theta(s, a))$. Given a collection of user preferences $\mathcal{D}_{\text{pref}}$, we learn θ by minimizing the following cross-entropy loss function [14, 10, 11]:

$$\mathcal{L}_{\text{pref}}(\theta) = - \sum_{\tau_i \succ \tau_j \in \mathcal{D}_{\text{pref}}} \log \left[\frac{\exp(\hat{J}_\theta(\tau_i))}{\exp(\hat{J}_\theta(\tau_i)) + \exp(\hat{J}_\theta(\tau_j))} \right]. \quad (1)$$

With image observations, rather than directly predicting rewards via $\hat{r}_\theta(s, a)$, we use an LSTM to generate reward predictions that integrate over a sequence of observations. The LSTM takes in a state sequence, and its final output is fed into the feedforward network \hat{r}_θ to predict the reward.

Learning a Dynamics Model. Given a dataset of observed state-action transitions, $\mathcal{D}_{\text{dyn}} = \{(s_i, a_i, s_{i+1})\}_{i=1}^M$, we learn a transition dynamics model $\hat{f}_\phi : \mathcal{S} \times \mathcal{A} \rightarrow \mathcal{S}$, parametrized by ϕ . We learn ϕ by minimizing the following loss:

$$\mathcal{L}_{\text{dyn}}(\phi) := \sum_{(s,a,s_{\text{next}}) \in \mathcal{D}_{\text{dyn}}} (s_{\text{next}} - \hat{f}_\phi(s, a))^2 + \lambda \|\phi\|^2, \quad (2)$$

where our forward dynamics network predicts the change in state, $\hat{f}_\phi^{\text{diff}}(s, a) := \hat{f}_\phi(s, a) - s$, and λ is a weight decay hyperparameter. We pre-process the data by normalizing it to have zero mean and unit variance along each dimension. When the observations are images, we adapt Stochastic Video Generation with a Learned Prior (SVG-LP) [17] to train a visual dynamics model.

This work leverages two methods for collecting the dynamics training dataset \mathcal{D}_{dyn} . The first is random agent-environment interaction, in which the agent samples its action space uniformly randomly over a series of trajectories beginning in different start states. However, in many domains, random agent-environment interaction may yield insufficient exploration. To collect diverse data for learning a dynamics model, we leverage random network distillation (RND) [12], a powerful approach for exploration in deep RL that provides reward bonuses based on the error of a neural network predicting the output of a randomly-initialized network. We gather a dataset of state-action transitions observed while training a Soft Actor Critic [25] policy using the RND bonus as the sole reward signal. In addition to using RND for dynamics pre-training, we integrate RND into our online learning pipeline as discussed below.

Pre-training with Suboptimal Demonstrations. Brown et al. [11] propose the D-REX algorithm, in which demonstration trajectories are automatically ranked based on the degree of noise used to generate them. We adapt D-REX to the model-based setting. Given a set of human demonstrations $\mathcal{D}_{\text{demo}}$, we train a behavior cloning policy $\pi_{BC} : \mathcal{S} \rightarrow \mathcal{A}$ on each state-action pair in $\mathcal{D}_{\text{demo}}$. Importantly, we roll out this policy inside the *learned dynamics model*. Simulated rollouts are generated with ϵ -greedy noise, such that the agent takes a uniformly random action with probability ϵ and follows π_{BC} otherwise. For trajectories τ_i and τ_j starting from the same initial state and generated with noise levels ϵ_i and ϵ_j , $\epsilon_i > \epsilon_j$, we automatically rank $\tau_j \succ \tau_i$. We also prefer any trajectory $\tau \in \mathcal{D}_{\text{demo}}$ over any trajectory generated by rolling out π_{BC} .

Model-Based RL. We adopt a model-based RL approach inspired by Chua et al. [15], leveraging the cross-entropy method (CEM) [40, 39] to plan with respect to learned reward and dynamics models. CEM maintains a distribution $\mathcal{N}(\boldsymbol{\mu}_i, \Sigma_i)$ in each CEM iteration i , from which the i^{th} population of m action sequences is sampled: $\{a_{1j}^{(i)}, \dots, a_{hj}^{(i)} \mid j = 1, \dots, m\}$, with planning horizon h . We then use the learned dynamics and rewards, \hat{f}_ϕ and \hat{r}_θ , to estimate the expected total reward $\tilde{R}_j^{(i)}$ of each action sequence, conditioned on a fixed start state $s_0 \in \mathcal{S}$: $\hat{s}_{1j}^{(i)} = \hat{f}_\phi(s_0, a_{1j}^{(i)})$, $\hat{s}_{2j}^{(i)} = \hat{f}_\phi(\hat{s}_{1j}^{(i)}, a_{2j}^{(i)})$, etc., and $\tilde{R}_j^{(i)} = \sum_{t=0}^{h-1} \hat{r}_\theta(\hat{s}_{tj}^{(i)}, a_{(t+1)j}^{(i)})$, where $\hat{s}_{0j}^{(i)} := s_0$. The m population members are then ranked according to their estimated rewards $\tilde{R}_j^{(i)}$, and the top $m_e < m$ population members are termed the *elites*. We take the mean and variance of the elites to refine the CEM distribution, obtaining $\mathcal{N}(\boldsymbol{\mu}_{i+1}, \Sigma_{i+1})$. To choose actions in the environment, we employ model predictive control (MPC), as in [15, 33]: we execute the first k actions of the action sequence given by the mean of the action distribution calculated in the final CEM iteration. Our experiments utilize $k = 1$.

We additionally leverage RND [12] to improve exploration. RND provides a prediction error signal $\hat{g}_\rho(s)$ at each state $s \in \mathcal{S}$, parameterized by ρ . Intuitively, areas with higher error $\hat{g}_\rho(s)$ have been explored less, and so $\hat{g}_\rho(s)$ functions as an exploration bonus. During CEM, we augment the expected reward: $\tilde{R}_j^{(i)} = \sum_{t=0}^{h-1} [\hat{r}_\theta(\hat{s}_{tj}^{(i)}, a_{(t+1)j}^{(i)}) + \lambda_{RND} \hat{g}_\rho(\hat{s}_{tj}^{(i)})]$, where λ_{RND} is a hyperparameter.

Active Model-Based Preference Query Generation. To efficiently generate pairwise preference queries without additional environment interaction, we form queries using trajectories from the CEM process, during which the learned dynamics \hat{f}_ϕ are used to roll out candidate action sequences. In selecting pairs of CEM trajectories to elicit preferences, we consider two main questions: (1) How can we generate a diverse pool $\mathcal{D}_{\text{traj}}$ of trajectories, e.g., so that the human is not forced to give preferences between overly-similar or otherwise limited choices? (2) Given a pool $\mathcal{D}_{\text{traj}}$ of candidate trajectories, how can we select which trajectory pairs are best to show to the human?

To address (1), we include trajectories from all CEM iterations in $\mathcal{D}_{\text{traj}}$. This ensures that $\mathcal{D}_{\text{traj}}$ contains diverse data, including from non-elite trajectories. Notably, constructing preference queries using only the final CEM iteration could force the human to compare overly-similar trajectories, leading to unreliable preference labels. At a randomly-selected time $t_{\text{keep}} \in \{1, \dots, T\}$ in each episode, we save $m_{\text{keep}} < m$ trajectories from each CEM iteration in $\mathcal{D}_{\text{traj}}$; these are randomly selected from the elites in the final CEM iteration and from among non-elites in previous iterations.

Algorithm 1: Model-based Preference-based Reinforcement Learning (MoP-RL)

```
1 Initialize parameters  $\theta, \phi$  of reward and dynamics networks  $\hat{r}_\theta$  and  $\hat{f}_\phi$ , respectively
2 Collect dataset  $\mathcal{D}_{\text{dyn}}$  of transitions in environment using exploration strategy (random or RND)
3 Optimize  $\mathcal{L}_{\text{dyn}}$  in (2) with respect to  $\phi$ 
4 Initialize  $\mathcal{D}_{\text{pref}} \leftarrow \emptyset$ 
5 Collect dataset  $\mathcal{D}_{\text{demo}}$  of human demonstrations
6 Initialize  $\hat{r}_\theta$  via model-based D-REX using  $\mathcal{D}_{\text{demo}}$  and using  $\hat{f}_\phi$  to roll out trajectories
7 for each episode  $k$  do
8   Initialize  $\mathcal{D}_{\text{traj}} \leftarrow \emptyset$ 
9    $t_{\text{keep}} \sim \mathcal{U}\{1, \dots, T\}$ 
10  for each timestep  $t \in \{1, \dots, T\}$  do
11     $s_t \leftarrow$  current state
12    Select optimal action sequence  $(a_t, \dots, a_{t+h-1})$  using CEM with  $\hat{f}_\phi, \hat{r}_\theta$ , and  $\hat{g}_\rho$ 
13    Execute  $a_t$  in the environment
14    if  $t = t_{\text{keep}}$  then
15       $\mathcal{D}_{\text{traj}} \leftarrow m_{\text{keep}}$  trajectories from each CEM iteration
16     $\{\tau_1^q, \tau_2^q \mid q = 1, \dots, N\} \leftarrow$  top  $N$  trajectory pairs in  $\mathcal{D}_{\text{traj}}$  according to info-gain (3)
17    for  $q = 1, \dots, N$  do
18      Query human for preference  $y$ 
19       $\mathcal{D}_{\text{pref}} \leftarrow \mathcal{D}_{\text{pref}} \cup \{(\tau_1^q, \tau_2^q, y)\}$ 
20    if  $k \%$  reward update frequency  $= 0$  then
21      Optimize  $\mathcal{L}_{\text{pref}}$  in (1) with respect to  $\theta$ 
22    if  $k \%$  RND update frequency  $= 0$  then
23      Update RND network  $g_\rho$  on visited states
```

We randomly choose a new t_{keep} in each episode so that across episodes, $\mathcal{D}_{\text{pref}}$ contains pairs of trajectories beginning in different states. For (2), we maximize the information gain [6, 5] to identify trajectory pairs in $\mathcal{D}_{\text{traj}}$ that are expected to be most informative about the human’s underlying reward r . We identify the N trajectory pairs $\{\tau_1^q, \tau_2^q \mid \tau_1^q, \tau_2^q \in \mathcal{D}_{\text{traj}}, q = 1, \dots, N\}$ with the highest mutual information $I(r; \mathbb{I}_{[\tau_1^q \succ \tau_2^q]} \mid \mathcal{D}_{\text{pref}})$ between their preference outcome and the unknown reward r [6, 5]:

$$I(r; \mathbb{I}_{[\tau_1 \succ \tau_2]} \mid \mathcal{D}_{\text{pref}}) = \left[H(\mathbb{I}_{[\tau_1 \succ \tau_2]} \mid \mathcal{D}_{\text{pref}}) - \mathbb{E}_{r \sim p(r \mid \mathcal{D}_{\text{pref}})} [H(\mathbb{I}_{[\tau_1 \succ \tau_2]} \mid r, \mathcal{D}_{\text{pref}})] \right], \quad (3)$$

where $\mathbb{I}_{[\tau_1 \succ \tau_2]} \in \{0, 1\}$ indicates the outcome of a preference query between τ_1 and τ_2 , $\mathcal{D}_{\text{pref}}$ is the pairwise preference dataset (so far), H is information entropy, and we use an ensemble of reward networks to estimate the posterior $p(r \mid \mathcal{D}_{\text{pref}})$. Algorithm 1 details the entire MoP-RL algorithm.

5 Experimental Results

5.1 Experiment Domains

Our experiments consider four simulation domains detailed below. For all domains, preferences are provided by a synthetic labeler; this simulated human does not make mistakes or provide preferences between trajectory pairs for which the reward difference falls below a threshold. Additional experiment details are provided in the Appendix.

Maze-LowDim. The agent must navigate a 2-dimensional maze to reach a goal location. The agent’s state is given by its (x, y) coordinates in the maze. The agent’s action is a vector $(f_x, f_y) \in \mathbb{R}^2$, $-f_{\text{max}} \leq f_x, f_y \leq f_{\text{max}}$, representing a force applied in each coordinate direction. The synthetic labeler provides preferences using a hand-specified underlying cost function, which gives higher preference first for reaching the far right wall and then the top-right corner.

Maze-Image. This environment uses the same maze, agent dynamics, and synthetic reward as Maze-LowDim; however, the agent observes an image of the environment (as in Fig. 2) at each step.

Assistive-Gym. We utilize a simplified version of the itch scratching task in the Assistive Gym [20] simulation environment (Fig. 3), in which a robot manipulator must position itself next to an itch on



Figure 3: Assistive Gym start (left) and goal (right) states.



Figure 4: MoP-RL trains a Hopper to perform a backflip via preference queries over learned dynamics.

a person’s arm and apply a target amount of force. We use a reduced state space containing 1) the vector difference between the robot end effector and itch location and 2) the amount of force applied by the end effector. The synthetic labeler prefers trajectories that bring the end effector close to the itch, and once sufficiently close, apply an amount of force below a threshold to the person’s arm.

Hopper. In the OpenAI Gym [8] Hopper environment, we aim to train the agent to perform a backflip. The state space $\mathcal{S} \subset \mathbb{R}^{11}$ consists of the angular positions and velocities of the Hopper’s 3 joints and the top of the robot, as well as the height of the hopper and the velocities of the x-coordinate and z-coordinate of the top. The action space $\mathcal{A} \subset \mathbb{R}^3$ consists of a torque applied to each of the 3 joints. Pairwise preferences over trajectories are given by a synthetic labeler with a hand-engineered reward function designed by Christiano et al. [14].

5.2 Performance Metrics and Algorithms Compared

Our experiments compare the performance of MoP-RL to PEBBLE [32], a state-of-the-art model-free PbRL algorithm. For each simulation domain, all algorithms learn from the same number of pairwise preferences. Performance is evaluated via the following metrics: 1. **Success rate** (Maze-LowDim, Maze-Image): percentage of times that the agent satisfies a goal condition. 2. **Average reward** (Assistive-Gym): ground truth reward over an entire episode, averaged over several rollouts.

In each environment, MoP-RL first trains a dynamics model. In Maze-LowDim, we collect dynamics training data via random environment interaction, while in the other domains—in which exploration is more challenging—we collect dynamics data via RND. Then, MoP-RL performs interactive reward learning, possibly with reward pre-training from demonstrations. The reward model \hat{r}_θ is a function of state and action in Assistive-Gym and Hopper, and of state only in both maze environments. PEBBLE performs an initial unsupervised exploration phase prior to reward learning. MoP-RL used 1000 trajectories to learn the dynamics model in Maze-LowDim, 2000 in Maze-Image, 2500 for Assistive-Gym, and 5000 for Hopper. PEBBLE used 150 trajectories in the unsupervised step in Maze-LowDim, 2000 or 5000 in Maze-Image (see Table 3), and 150 in Assistive-Gym.

Algorithm	Training Rollouts	Success Rate
PEBBLE	50	6.3%
PEBBLE	100	81.3%
PEBBLE	200	100.0%
MoP-RL (w/o demos)	18	0.0%
MoP-RL (w/o demos)	24	56.25%
MoP-RL (w/o demos)	30	100.0%
MoP-RL (w/ 2 demos)	18	100.0%
MoP-RL (w/ 2 demos)	24	100.0%
MoP-RL (w/ 2 demos)	30	100.0%

Table 1: **Performance on Maze-LowDim Environment.** We report the numbers of unsupervised and training rollouts and the success rate (over 16 rollouts) for each method when trained with 60 preference queries.

Algorithm	Training Rollouts	Average Reward
PEBBLE	100	-46.1 \pm 1.36
MoP-RL	8	-26.9 \pm 6.82

Table 2: **Performance on Assistive-Gym Itch Scratching Environment.** We report the numbers of unsupervised and training rollouts and the average reward (mean \pm standard error over 4 rollouts) for each method compared. Both methods were trained with 80 preference queries.

Table 3: **Performance on Maze-Image Environment.** We report the numbers of unsupervised and training rollouts and the success rate (over 16 rollouts) for each method compared. Both methods were trained with 1000 preference queries.

Algorithm	Unsupervised Rollouts	Training Rollouts	Success Rate
PEBBLE	2000	3300	0.0%
PEBBLE	5000	3300	0.0%
MoP-RL (w/o demos)	2000	800	25.0%
MoP-RL (w/ 2 demos)	2000	800	68.8%

5.3 Results

We hypothesize that MoP-RL will require fewer environmental interactions in comparison to model-free RL, while achieving similar or better performance. We compare MoP-RL and PEBBLE [32] in the Maze-LowDim, Maze-Image, and Assistive-Gym Itch Scratching tasks.

Maze-LowDim. Table 1 shows results for the Maze-LowDim environment. We see that PEBBLE requires a large number of rollouts to learn the reward function accurately enough to successfully navigate the maze. By contrast, MoP-RL is much more sample efficient. We also observe that pre-training the reward network using the demonstrations significantly speeds up online preference learning, requiring fewer trajectories to successfully complete the task.

Maze-Image. Table 3 shows results for the Maze-Image environment. We see that MoP-RL outperforms PEBBLE, even when PEBBLE is given significantly more unsupervised access to the environment. Prior work [32] only evaluates PEBBLE on low-dimensional reward learning tasks. We adapted the author’s implementation of PEBBLE to allow an image-based reward function and use the same reward function architecture for both PEBBLE and MoP-RL. However, our results demonstrate that PEBBLE struggles in high-dimensional visual domains. Furthermore, we see that adding pre-training with a small number of demonstrations, namely ten demonstrations, can significantly improve reward learning, leading to improved task success by first learning a rough estimate of the reward function and then fine-tuning that estimate via model-based preference queries.

Assistive Gym. Table 2 shows the results for the itching task from Assistive Gym. MoP-RL is able to reach a higher reward in this environment in performing this task.

The above experiments demonstrate that MoP-RL requires significantly fewer environment interaction steps than PEBBLE to learn a reward function. MoP-RL also enables dynamics model pre-training to be performed separately from preference learning; in particular, unlike a learned reward function, learned dynamics can be re-used to safely and efficiently learn the preferences of multiple users.

Hopper Backflip. Inspired by previous model-free PbRL results [14], we demonstrate that MoP-RL can train the OpenAI Gym Hopper to perform a backflip via preference queries over a learned dynamics model. An example learned backflip is displayed in Figure 4, suggesting that MoP-RL can learn to perform novel behaviors for which designing a hand-crafted reward function is difficult.

6 Discussion and Limitations

This work introduces MoP-RL, a model-based approach to preference-based RL. We demonstrate that dynamics modeling is uniquely suited for preference-based learning, since learned dynamics can be used to generate pairwise preference queries without environment interaction. In addition, MoP-RL performs robust exploration through random network distillation and information gain maximization techniques, and combines multiple human interaction modalities by integrating preference learning with model-based reward pre-training from demonstrations. Limitations of this study include that we synthetically generated all pairwise preferences, we do not consider noisy preference data, and we have not quantified the safety benefits of MoP-RL. Thus, in future work, we plan to evaluate MoP-RL in a human user study and consider safety-critical domains. We are also excited to explore physical robotics applications of MoP-RL, in which environment interactions are expensive, while different human users could have varying robot interaction preferences.

References

- [1] Brenna D Argall, Sonia Chernova, Manuela Veloso, and Brett Browning. A survey of robot learning from demonstration. *Robotics and autonomous systems*, 57(5):469–483, 2009.
- [2] Nir Baram, Oron Anshel, Itai Caspi, and Shie Mannor. End-to-end differentiable adversarial imitation learning. In *International Conference on Machine Learning*, pages 390–399. PMLR, 2017.
- [3] Nir Baram, Oron Anshel, and Shie Mannor. Model-based adversarial imitation learning. *arXiv preprint arXiv:1612.02179*, 2016.
- [4] Sarah Bechtler, Yixin Lin, Akshara Rai, Ludovic Righetti, and Franziska Meier. Curious iLQR: Resolving uncertainty in model-based RL. In *Conference on Robot Learning*, pages 162–171. PMLR, 2020.
- [5] Erdem Biyik, Nicolas Huynh, Mykel Kochenderfer, and Dorsa Sadigh. Active preference-based Gaussian process regression for reward learning. In *Robotics: Science and Systems*, 2020.
- [6] Erdem Biyik, Malayandi Palan, Nicholas C Landolfi, Dylan P Losey, Dorsa Sadigh, et al. Asking easy questions: A user-friendly approach to active reward learning. In *Conference on Robot Learning*, pages 1177–1190. PMLR, 2020.
- [7] Zdravko I Botev, Dirk P Kroese, Reuven Y Rubinstein, and Pierre L’Ecuyer. The cross-entropy method for optimization. In *Handbook of statistics*, volume 31, pages 35–59. Elsevier, 2013.
- [8] Greg Brockman, Vicki Cheung, Ludwig Pettersson, Jonas Schneider, John Schulman, Jie Tang, and Wojciech Zaremba. Openai gym, 2016.
- [9] Daniel Brown, Russell Coleman, Ravi Srinivasan, and Scott Niekum. Safe imitation learning via fast Bayesian reward inference from preferences. In *International Conference on Machine Learning*, pages 1165–1177. PMLR, 2020.
- [10] Daniel Brown, Wonjoon Goo, Prabhat Nagarajan, and Scott Niekum. Extrapolating beyond sub-optimal demonstrations via inverse reinforcement learning from observations. In *International Conference on Machine Learning*, pages 783–792. PMLR, 2019.
- [11] Daniel S Brown, Wonjoon Goo, and Scott Niekum. Better-than-demonstrator imitation learning via automatically-ranked demonstrations. In *Conference on robot learning*, pages 330–359. PMLR, 2020.
- [12] Yuri Burda, Harrison Edwards, Amos Storkey, and Oleg Klimov. Exploration by random network distillation. In *Seventh International Conference on Learning Representations*, pages 1–17, 2019.
- [13] Letian Chen, Rohan Paleja, and Matthew Gombolay. Learning from suboptimal demonstration via self-supervised reward regression. In *Conference on robot learning*, pages 1262–1277. PMLR, 2021.
- [14] Paul F Christiano, Jan Leike, Tom B Brown, Miljan Martic, Shane Legg, and Dario Amodei. Deep reinforcement learning from human preferences. In *NIPS*, 2017.
- [15] Kurtland Chua, Roberto Calandra, Rowan McAllister, and Sergey Levine. Deep reinforcement learning in a handful of trials using probabilistic dynamics models. *Advances in neural information processing systems*, 31, 2018.
- [16] Caleb Chuck, Michael Laskey, Sanjay Krishnan, Ruta Joshi, Roy Fox, and Ken Goldberg. Statistical data cleaning for deep learning of automation tasks from demonstrations. In *2017 13th IEEE Conference on Automation Science and Engineering (CASE)*, pages 1142–1149. IEEE, 2017.
- [17] Emily Denton and Rob Fergus. Stochastic video generation with a learned prior. In *International conference on machine learning*, pages 1174–1183. PMLR, 2018.
- [18] Frederik Ebert, Chelsea Finn, Sudeep Dasari, Annie Xie, Alex Lee, and Sergey Levine. Visual foresight: Model-based deep reinforcement learning for vision-based robotic control. *arXiv preprint arXiv:1812.00568*, 2018.
- [19] Ashley Edwards, Himanshu Sahni, Yannick Schroecker, and Charles Isbell. Imitating latent policies from observation. In *International conference on machine learning*, pages 1755–1763. PMLR, 2019.

- [20] Zackory Erickson, Vamsee Gangaram, Ariel Kapusta, C Karen Liu, and Charles C Kemp. Assistive Gym: A physics simulation framework for assistive robotics. In *2020 IEEE International Conference on Robotics and Automation (ICRA)*, pages 10169–10176. IEEE, 2020.
- [21] Chelsea Finn and Sergey Levine. Deep visual foresight for planning robot motion. In *2017 IEEE International Conference on Robotics and Automation (ICRA)*, pages 2786–2793. IEEE, 2017.
- [22] Chelsea Finn, Sergey Levine, and Pieter Abbeel. Guided cost learning: Deep inverse optimal control via policy optimization. In *International conference on machine learning*, pages 49–58. PMLR, 2016.
- [23] Artem Gritsenko and Dmitry Berenson. Learning cost functions for motion planning from human preferences. In *Proceedings of the IROS 2014 Workshop on Machine Learning in Planning and Control of Robot Motion*, volume 1, pages 48–6, 2014.
- [24] Steffen Grünewälder, Guy Lever, Luca Baldassarre, Massimiliano Pontil, and Arthur Gretton. Modelling transition dynamics in MDPs with RKHS embeddings. In *Proceedings of the 29th International Conference on Machine Learning*, pages 1603–1610, 2012.
- [25] Tuomas Haarnoja, Aurick Zhou, Pieter Abbeel, and Sergey Levine. Soft actor-critic: Off-policy maximum entropy deep reinforcement learning with a stochastic actor. In *International conference on machine learning*, pages 1861–1870. PMLR, 2018.
- [26] Danijar Hafner, Timothy Lillicrap, Ian Fischer, Ruben Villegas, David Ha, Honglak Lee, and James Davidson. Learning latent dynamics for planning from pixels. In *International conference on machine learning*, pages 2555–2565. PMLR, 2019.
- [27] Borja Ibarz, Jan Leike, Tobias Pohlen, Geoffrey Irving, Shane Legg, and Dario Amodei. Reward learning from human preferences and demonstrations in Atari. *arXiv preprint arXiv:1811.06521*, 2018.
- [28] Ashesh Jain, Shikhar Sharma, Thorsten Joachims, and Ashutosh Saxena. Learning preferences for manipulation tasks from online coactive feedback. *The International Journal of Robotics Research*, 34(10):1296–1313, 2015.
- [29] Łukasz Kaiser, Mohammad Babaeizadeh, Piotr Miłoś, Błażej Osipiński, Roy H Campbell, Konrad Czechowski, Dumitru Erhan, Chelsea Finn, Piotr Kozakowski, Sergey Levine, et al. Model based reinforcement learning for Atari. In *International Conference on Learning Representations*, 2019.
- [30] Rahul Kidambi, Jonathan Chang, and Wen Sun. Mobile: Model-based imitation learning from observation alone. *Advances in Neural Information Processing Systems*, 34, 2021.
- [31] J Zico Kolter and Gaurav Manek. Learning stable deep dynamics models. *Advances in neural information processing systems*, 32, 2019.
- [32] Kimin Lee, Laura Smith, and Pieter Abbeel. PEBBLE: Feedback-efficient interactive reinforcement learning via relabeling experience and unsupervised pre-training. *arXiv preprint arXiv:2106.05091*, 2021.
- [33] Kendall Lowrey, Aravind Rajeswaran, Sham Kakade, Emanuel Todorov, and Igor Mordatch. Plan online, learn offline: Efficient learning and exploration via model-based control. In *International Conference on Learning Representations*, 2018.
- [34] Ajay Mandlekar, Danfei Xu, Josiah Wong, Soroush Nasiriany, Chen Wang, Rohun Kulkarni, Li Fei-Fei, Silvio Savarese, Yuke Zhu, and Roberto Martín-Martín. What matters in learning from offline human demonstrations for robot manipulation. *arXiv preprint arXiv:2108.03298*, 2021.
- [35] Anusha Nagabandi, Kurt Konolige, Sergey Levine, and Vikash Kumar. Deep dynamics models for learning dexterous manipulation. In *Conference on Robot Learning*, pages 1101–1112. PMLR, 2020.
- [36] Duy Nguyen-Tuong and Jan Peters. Model learning for robot control: a survey. *Cognitive processing*, 12(4):319–340, 2011.
- [37] Masashi Okada and Tadahiro Taniguchi. Variational inference mpc for Bayesian model-based reinforcement learning. In *Conference on Robot Learning*, pages 258–272. PMLR, 2020.

- [38] Siddharth Reddy, Anca Dragan, Sergey Levine, Shane Legg, and Jan Leike. Learning human objectives by evaluating hypothetical behavior. In *International Conference on Machine Learning*, pages 8020–8029. PMLR, 2020.
- [39] R. Rubinstein and D. Kroese. *The Cross-Entropy Method: A Unified Approach to Combinatorial Optimization, Monte-Carlo Simulation, and Machine Learning*. Springer-Verlag, 2004.
- [40] Reuven Rubinstein. The Cross-Entropy Method for Combinatorial and Continuous Optimization. *Methodology And Computing In Applied Probability*, 1999.
- [41] Dorsa Sadigh, Anca D Dragan, Shankar Sastry, and Sanjit A Seshia. Active preference-based learning of reward functions. In *Robotics: Science and Systems*, 2017.
- [42] Thomas George Thuruthel, Egidio Falotico, Federico Renda, and Cecilia Laschi. Learning dynamic models for open loop predictive control of soft robotic manipulators. *Bioinspiration & biomimetics*, 12(6):066003, 2017.
- [43] Faraz Torabi, Garrett Warnell, and Peter Stone. Behavioral cloning from observation. In *Proceedings of the 27th International Joint Conference on Artificial Intelligence*, pages 4950–4957, 2018.
- [44] Rishi Veerapaneni, John D Co-Reyes, Michael Chang, Michael Janner, Chelsea Finn, Jiajun Wu, Joshua Tenenbaum, and Sergey Levine. Entity abstraction in visual model-based reinforcement learning. In *Conference on Robot Learning*, pages 1439–1456. PMLR, 2020.
- [45] Sean J Wang, Samuel Triest, Wenshan Wang, Sebastian Scherer, and Aaron Johnson. Rough terrain navigation using divergence constrained model-based reinforcement learning. In *5th Annual Conference on Robot Learning*, 2021.
- [46] Grady Williams, Andrew Aldrich, and Evangelos Theodorou. Model predictive path integral control using covariance variable importance sampling. *arXiv preprint arXiv:1509.01149*, 2015.
- [47] Aaron Wilson, Alan Fern, and Prasad Tadepalli. A Bayesian approach for policy learning from trajectory preference queries. *Advances in neural information processing systems*, 25, 2012.
- [48] Christian Wirth, Riad Akrou, Gerhard Neumann, Johannes Fürnkranz, et al. A survey of preference-based reinforcement learning methods. *Journal of Machine Learning Research*, 18(136):1–46, 2017.
- [49] Christian Wirth and Johannes Fürnkranz. On learning from game annotations. *IEEE Transactions on Computational Intelligence and AI in Games*, 7(3):304–316, 2014.
- [50] Christian Wirth, Johannes Fürnkranz, and Gerhard Neumann. Model-free preference-based reinforcement learning. In *Thirtieth AAAI Conference on Artificial Intelligence*, 2016.
- [51] Alan Wu, AJ Piergiovanni, and Michael S Ryoo. Model-based behavioral cloning with future image similarity learning. In *Conference on Robot Learning*, pages 1062–1077. PMLR, 2020.
- [52] Bohan Wu, Suraj Nair, Li Fei-Fei, and Chelsea Finn. Example-driven model-based reinforcement learning for solving long-horizon visuomotor tasks. In *5th Annual Conference on Robot Learning*, 2021.
- [53] Yunkun Xu, Zhenyu Liu, Guifang Duan, Jiangcheng Zhu, Xiaolong Bai, and Jianrong Tan. Look before you leap: Safe model-based reinforcement learning with human intervention. In *Conference on Robot Learning*, pages 332–341. PMLR, 2022.
- [54] Tianhe Yu, Garrett Thomas, Lantao Yu, Stefano Ermon, James Y Zou, Sergey Levine, Chelsea Finn, and Tengyu Ma. Mopo: Model-based offline policy optimization. *Advances in Neural Information Processing Systems*, 33:14129–14142, 2020.
- [55] Marvin Zhang, Sharad Vikram, Laura Smith, Pieter Abbeel, Matthew Johnson, and Sergey Levine. Solar: Deep structured representations for model-based reinforcement learning. In *International Conference on Machine Learning*, pages 7444–7453. PMLR, 2019.
- [56] Yunzhi Zhang, Ignasi Clavera, Boren Tsai, and Pieter Abbeel. Asynchronous methods for model-based reinforcement learning. In *Conference on Robot Learning*, pages 1338–1347. PMLR, 2020.
- [57] Matt Zucker, J Andrew Bagnell, Christopher G Atkeson, and James Kuffner. An optimization approach to rough terrain locomotion. In *2010 IEEE International Conference on Robotics and Automation*, pages 3589–3595. IEEE, 2010.

Checklist

A Appendix: Additional Experiment Details

Hyperparameters used in our experiments are detailed below in Table 4.

Hyperparameter	Value
RND weight, λ_{RND}	0.1
Dynamics weight decay, λ	0.01
Size of reward ensemble	3
Dynamics learning rate	2e-3
Reward learning rate	2e-4
CEM population size, m	200
CEM elites, m_e	20
CEM iterations	5

Table 4: MoP-RL hyperparameters for low-dimensional experiments.

Each training executed using a single NVIDIA GeForce RTX 2070 GPU and lasted approximately 1-2 hours.